GPS/STORM—GPS Sensing of Atmospheric Water Vapor for Meteorology

CHRISTIAN ROCKEN, TERESA VAN HOVE, JAMES JOHNSON, FRED SOLHEIM, AND RANDOLPH WARE

University Navstar Consortium/UCAR, Boulder, Colorado

MIKE BEVIS, STEVE CHISWELL, AND STEVE BUSINGER

University of Hawaii, Honolulu, Hawaii

(Manuscript received 16 May 1994, in final form 16 November 1994)

ABSTRACT

Atmospheric water vapor was measured with six Global Positioning System (GPS) receivers for 1 month at sites in Colorado, Kansas, and Oklahoma. During the time of the experiment, from 7 May to 2 June 1993, the area experienced severe weather. The experiment, called "GPS/STORM," used GPS signals to sense water vapor and tested the accuracy of the method for meteorological applications. Zenith wet delay and precipitable water (PW) were estimated, relative to Platteville, Colorado, every 30 min at five sites. At three of these five sites the authors compared GPS estimates of PW to water vapor radiometer (WVR) measurements. GPS and WVR estimates agree to 1–2 mm rms. For GPS/STORM site spacing of 500–900 km, high-accuracy GPS satellite orbits are required to estimate 1–2-mm-level PW. Broadcast orbits do not have sufficient accuracy. It is possible, however, to estimate orbit improvements simultaneously with PW. Therefore, it is feasible that future meteorological GPS networks provide near-real-time high-resolution PW for weather forecasting.

1. Introduction

Because the GPS signal is sensitive to the refractive index of the atmosphere, and because this index is a function of pressure, temperature, and moisture, GPS can be used directly for sensing properties of the atmosphere. Small amounts of atmospheric water vapor significantly affect GPS signal propagation velocities. Thus, GPS is especially well suited for sensing atmospheric water vapor, which plays a major role in atmospheric processes ranging from global climate change to micrometeorology.

Atmospheric scientists have developed a variety of means to measure the vertical and horizontal distribution of water vapor. The cornerstone of the operational analysis and prediction system at the National Meteorological Center, and at similar operational weather forecast centers worldwide, is the expendable radiosonde. The cost of radiosondes at $250 per release limits the number of launches to twice daily (0000 and 1200 UTC) at a limited number of stations. Because of these restrictions, radiosonde measurements inadequately resolve the temporal and spatial variability of water vapor.

Ground-based water vapor radiometers (WVRs) are instruments that scan the sky and measure the microwave radiation emitted by atmospheric water vapor. The frequency dependence of sky brightness temperature enables the simultaneous estimation of integrated water vapor (IWV) and integrated liquid water along each line of sight in the scanning pattern. Most meteorologists are more familiar with space-based, downward-looking WVRs. While upward-looking WVRs measure water vapor emission lines against the cold background of space, downward-looking WVRs measure the corresponding absorption lines in the radiation from the hot background provided by the earth. The recovery of IWV by space-based WVRs is greatly complicated over land by the variability of land surface temperature. A similar problem is posed by clouds. For this reason, satellite-based WVRs tend to be more useful over the oceans than over land, and their usefulness is degraded in the presence of clouds. Ground-based WVRs are not affected by light or moderate cloud cover, though their performance may be degraded in the presence of heavy clouds, and very few of these devices provide useful data when it is raining. Satellite-based WVRs provide good spatial coverage but poor coverage in time, whereas ground-based WVRs have the opposite characteristics (Bevis et al. 1992).

Satellite soundings showed great promise in the 1970s. However, with improvement to the database from aircraft observations, their contribution to forecasting in the Northern Hemisphere is limited due to inadequate vertical resolution. In the Southern Hemisphere, with significantly less air traffic, these obser-

Corresponding author address: Dr. Christian Rocken, UNAVCO, University NAVSTAR Consortium, P.O. Box 3000, Boulder, CO 80307-3000.

vations are still a useful data supplement. Ground-based GPS observations of atmospheric water vapor made on small islands and offshore oil platforms can be used to calibrate space-based radiometers—thus, supporting and potentially improving the existing satellite observation and forecasting systems.

Recently, the use of GPS signals has been suggested to supplement the existing weather-monitoring systems. Ground-based (Bevis et al. 1992; Rocken et al. 1993) and space-based systems (Yuan et al. 1993) both hold the potential to provide valuable data for weather forecasting and climate research. Kuo et al. (1993) have shown that integrated water vapor and water vapor profile data can both aid weather forecasting. Taken together, existing systems and new GPS systems hold promise to provide the detail necessary for significant increases in forecast accuracy.

2. Ground-based GPS systems for meteorology

GPS microwave frequency signals are slowed by the earth's ionosphere and neutral atmosphere. Ionospheric delays are highly variable, ranging from 1 to 15 m in the zenith direction. These delays can be corrected with millimeter accuracy, because GPS signals are transmitted at two frequencies, and because it is known that the ionospheric delay is approximately proportional to the inverse square of the signal frequency (Spilker 1980).

Neutral atmospheric zenith delays are approximately 250 cm at sea level and have two components. Wet delay is caused by atmospheric water vapor, and dry or hydrostatic delay by all other atmospheric constituents. The hydrostatic delay of a zenith GPS signal traveling to an atmospheric depth of 1000 mb is approximately 230 cm. Assuming hydrostatic equilibrium, this delay can be predicted to better than 1 mm with surface pressure measurement accuracies of 0.5 mb. The error introduced by the assumption of hydrostatic equilibrium depends on winds and topology but is typically of the order of 0.01%. This corresponds to 0.2 mm in zenith delay. Extreme conditions may cause an error of several millimeters (Elgered 1993).

Wet GPS signal delay ranges from 0 to 40 cm in the zenith direction. Zenith wet delay (ZWD) is highly variable and cannot be accurately predicted from surface observations. Precipitable water (PW) is the depth of water that would result if all atmospheric water vapor in a vertical column of air were condensed to liquid. One centimeter of PW causes approximately 6.5 cm of GPS wet signal delay [see Eq. (11)]. This 6.5-fold "amplification" effect is important for accurate PW measurement with GPS.

Zenith delays can be mapped to lower observation angles by use of mapping functions (i.e., Davis et al. 1985; Saastamoinen 1972; Hopfield 1971). Mapping functions describe the approximately "1/sin(elevation angle)" dependence of the delay and include additional correction terms for the bending of the ray and for the sphericity of earth. Mapping functions and accurate pressure measurements provide millimeter-accurate hydrostatic delay corrections for observations as low as 15°.

Wet delay can be determined directly from GPS observations. Assume that the geometric distance and direction from a station to a GPS satellite are known. Assume further that GPS provides a range measurement that can be corrected for ionospheric (using dual-frequency data) and hydrostatic delay (using pressure data and mapping function). If this corrected GPS observation is modeled as the geometric range, then the "observed-minus-computed" residual is the wet delay in the direction of the GPS satellite. Because the elevation angle of the GPS satellite is known, the wet delay in the zenith direction can be computed, and simultaneous measurements from multiple GPS satellites in different directions can be averaged.

This description of estimating wet delay with GPS is greatly simplified. Several characteristics of the GPS phase measurement complicate the estimation. First, when the observed-minus-computed residual is calculated, the residual is not only biased by the wet delay. Even if we assume that station position and satellite orbits are known with negligible uncertainty, there are still biases due to GPS satellite clocks, the receiver clock, and the integer carrier phase cycle ambiguities. These biases have to be corrected before the wet delay can be measured directly with GPS.

Clock errors are usually cancelled by a technique called double-differencing (Remondi 1984) or equivalent techniques (Tralli and Lichten 1990). Satellite clock errors are cancelled by forming the so-called single differences of simultaneous measurements from the same satellite by two receivers. Single differences are nearly free of satellite clock errors but they are still affected by receiver clock errors. The difference between two single differences for two satellites is called the double difference and cancels receiver clock errors. This method of removing clock errors is the main reason why estimation of tropospheric parameters using GPS is a relative measurement between two points.

Doubly differenced phase observations are virtually free of clock errors but have carrier phase ambiguities. These ambiguities have two important properties. While the GPS receiver maintains signal lock, cycle ambiguities remain constant and they are integer multiples of GPS carrier wavelengths. GPS software distinguishes between carrier phase ambiguities and wet delay because the former remains constant while the latter changes roughly as 1/sin(satellite elevation angle). Thus, ambiguities and zenith wet delay can be estimated simultaneously by GPS least-squares adjustment (Rothacher 1992) or Kalman filter parameter estimation (Tralli et al. 1992). It is possible to estimate tropospheric delay parameters with temporal resolution ranging from several minutes to hours.

Combined wet and hydrostatic zenith delay can, thus, be estimated for each station equipped with a GPS receiver. If the station is also equipped with a good barometer for independent estimation of the hydrostatic delay, it is possible to estimate zenith wet delay. Delay estimation at every GPS station is called absolute tropospheric estimation. Estimation of differences in delay between two stations is called relative or differential estimation.

For GPS networks with apertures (station spacing) smaller than about 500 km, both the deterministic (least squares) and Kalman filtering techniques used to estimate zenith delay are more sensitive to relative rather than absolute delays (Rocken et al. 1993). This situation arises because a GPS satellite observed from two or more receivers is viewed at almost identical elevation angles, causing delay estimates to be highly correlated. ZWD and, hence, PW derived from a small network are subject to an unknown bias at each epoch. The value of this bias is constant across the whole network (i.e., the bias varies in time but not in space). There are several possible approaches to estimating this bias, a task known as levering. One is to measure PW with a WVR at a single reference site and use the GPS data to estimate PW relative to this reference site at any number of so-called secondary sites. This method of differential estimation depends on reliable WVR data from the reference site. Other levering approaches are under development. The most attractive approach to eliminate the need for an independent measurement of PW at a reference site is to incorporate a few GPS stations that introduce baselines significantly longer than 500 km. Provided that good orbit information is available, absolute ZWD and, therefore, absolute PW can then be computed from the GPS observations alone.

In the following, we first describe absolute, then differential tropospheric estimation with GPS, and discuss the main errors affecting these techniques.

a. Absolute tropospheric estimation

Absolute estimation requires one site separated by 500 km or more from a network of GPS receivers. Wet delay can be computed from barometric and GPS data only. If the hydrostatic delay is known a priori from pressure measurements, GPS estimates the wet delay as

$$ZD_{GPS} = (ZD_{actual} - ZD_{apriori}) + \delta ZD_{GPS}, \quad (1)$$

where ZD_{GPS} is the GPS estimated zenith delay, ZD_{actual} the tropospheric zenith delay, $ZD_{apriori}$ the applied a priori correction, and δZD_{GPS} is the error of the GPS estimate. The delay has a hydrostatic and a wet component:

$$ZD_{actual} = ZD_{hydrostatic} + ZD_{wet}, \quad (2)$$

where $ZD_{hydrostatic}$ and ZD_{wet} are the true values of the hydrostatic and wet delays. The a priori estimate of the hydrostatic delay has an error $\delta ZD_{hydrostatic}$ due to barometer calibration errors and errors in relating pressure observations to delays:

$$ZD_{apriori} = ZD_{hydrostatic} + \delta ZD_{hydrostatic}. \quad (3)$$

Therefore, we get

$$ZD_{GPS} = ZD_{wet} + \delta ZD_{hydrostatic} + \delta ZD_{GPS}. \quad (4)$$

Absolute estimation is affected by hydrostatic delay errors at one site $\delta ZD_{hydrostatic}$ and by GPS errors. The error of the estimated wet delay is, therefore,

$$\delta ZD = (\delta ZD^2_{hydrostatic} + \delta ZD^2_{GPS})^{1/2}. \quad (5)$$

The zenith hydrostatic delay correction is typically good to about 1 mm. The error of the absolute GPS estimate of delay δZD_{GPS} has been shown in data simulations to be currently no better than approximately 15 mm (Rocken et al. 1993), corresponding to an uncertainty in the precipitable water of about 2 mm. Efforts to improve the algorithms used for absolute estimation are currently under way.

b. Differential tropospheric estimation

This study presents tropospheric delays that were estimated relative to a reference site where hydrostatic delay from a barometer plus wet delay from a WVR were applied a priori. Only hydrostatic corrections were applied at secondary GPS sites. Thus, the GPS estimated differential tropospheric delay is the wet delay at the secondary sites. Differentially estimated delay ZD_{GPS} can be written as

$$ZD_{GPS} = (ZD_{actual} - ZD_{apriori})_{ref} - (ZD_{actual} - ZD_{apriori})_{secondary}. \quad (6)$$

The a priori delay at the reference site is

$$ZD_{apriori_{ref}} = (ZD_{hydrostatic} + \delta ZD_{hydrostatic} + ZD_{wet} + \delta ZD_{wet})_{ref}, \quad (7)$$

and at the secondary site the a priori delay is

$$ZD_{apriori_{secondary}} = (ZD_{hydrostatic} + \delta ZD_{hydrostatic})_{secondary}. \quad (8)$$

If the total delay for the reference site and the hydrostatic delay for the secondary site are known a priori, the tropospheric GPS estimate can be written as

$$ZD_{GPS} = (\delta ZD_{hydrostatic} + \delta ZD_{wet})_{ref} + (ZD_{wet} + \delta ZD_{hydrostatic})_{secondary} + \delta ZD_{GPS}, \quad (9)$$

where δZD_{wet} is the error of the a priori estimation of the wet delay at the reference site. If the a priori wet delay is estimated with a WVR, δZD_{wet} is due to ra-

diometer errors. The differential technique can estimate the wet delay at any secondary site. This estimation is affected by several errors, one of which is the error in the GPS estimation itself. The other errors stem from uncertainties in the a priori values of wet and hydrostatic delay. The error of the estimated zenith wet delay can be computed from

$$\delta ZD = [(\delta ZD^2_{\text{hydrostatic}} + \delta ZD^2_{\text{GPS}})_{\text{secondary}} + (\delta ZD^2_{\text{hydrostatic}} + \delta ZD^2_{\text{wet}})_{\text{ref}}]^{1/2}. \quad (10)$$

The differential zenith delay error from GPS δZD_{GPS}, due to orbit errors, signal multipath, and phase noise for this experiment is 5 mm or less (Rocken et al. 1993; Herring 1986). In addition, the wet delay error δZD_{wet} due to the WVR is approximately 6 mm (Gary et al. 1985; Westwater et al. 1989). Most of this error is due to uncertainties in converting radiometric observations to wet delay. Only about 2 mm are believed to be caused by instrumental errors (Solheim 1993; Ware et al. 1993). Using the same hydrostatic delay errors as before, the total uncertainty in the zenith wet delay is about 8 mm, corresponding to 1.2 mm in precipitable water.

c. *Absolute versus differential techniques*

The main advantage of the absolute estimation technique is that it requires only GPS receivers and barometers. The main disadvantage is that it does not work over short distances.

The main advantages of the differential technique are that it works over any distance and that it is potentially the most accurate method for determining the zenith wet delay with GPS. This method can work for small (<100 km) networks using on-line broadcast GPS orbits in near-real time. The main disadvantage is that at least one independent measurement of the zenith wet delay is required. This measurement can be done with a WVR. WVR measurement errors at the reference site affect all secondary stations. To estimate the wet delay at a secondary site, five different datasets must be available: barometric pressure and GPS data from the reference and secondary sites plus WVR data from the reference site. If any of these five datasets are in error or missing, faulty or missing zenith wet delay estimates are the result.

d. *Estimating zenith precipitable water from wet delay*

GPS estimated zenith wet delay can be converted to zenith PW without incurring any significant additional errors using the equation (Bevis et al. 1992)

$$PW = \Pi ZD_{GPS}. \quad (11)$$

The factor Π is approximately 0.15. This value varies with location, elevation, and season by as much as 20% but can be determined to about 2% if Π is computed as a function of surface temperature. The factor Π can be determined to 1%, if data from numerical weather models are used (Bevis et al. 1994). In the study presented here, we computed Π as a function of surface temperature according to the equation

$$\Pi = 10^6 \left[R_v \left(\frac{k_3}{T_m} + k'_2 \right) \right]^{-1}, \quad (12)$$

where $R_v = 461.495$ J kg^{-1} K^{-1} is the specific gas constant for water vapor. The weighted mean temperature of the wet part of the atmosphere is T_m, which can be estimated as a function of surface temperature T_s as $T_m = 70.2 + 0.72T_s$ (Bevis et al. 1992). The remaining constants in the above equation are

$$k'_2 = k_2 - mk_1, \quad (13)$$

where m is M_w/M_d, the ratio of the molar masses of water vapor and dry air. The physical constants k_1, k_2, and k_3 (for this study we used $k'_2 = 22$ K mb^{-1} and $k_3 = 3.739 \times 10^5$ K^2 mb^{-1}) are from the formula for atmospheric refractivity N (Smith and Weintraub 1953; Boudouris 1963):

$$N = k_1 \left(\frac{P_d}{T} \right) + k_2 \left(\frac{P_v}{T} \right) + k_3 \left(\frac{P_v}{T^2} \right), \quad (14)$$

where P_d and P_v are the partial pressures of dry air and water vapor, respectively, and T is the absolute temperature.

3. GPS/STORM experiment description

Six sites were equipped with GPS and surface meteorological equipment. Four of the sites also had WVRs. Three of these WVRs were Radiometrics™ instruments (Solheim 1993), and one was a NOAA WVR (Westwater 1978). Two of the Radiometrics™ instruments were installed and operated by the UNAVCO/NCSU team. One was operated by the Atmospheric Radiation Measurement (ARM) project at the Department of Energy's Southern Great Plains Cloud and Radiation Testbed (CART) site near Lamont, Oklahoma.

All GPS receivers were Trimble™ 4000 SSE P-code receivers. GPS antennas were mounted approximately 3 m high atop stable fence posts at NOAA wind profiler sites and atop a trailer at the CART site. All receivers logged data for 22 h each day at a sampling interval of 30 s. Data were downloaded once per day automatically to a PC at the site. During the 2-h window when the receivers were not logging data, the site status was checked by phone. Data that had been downloaded to the PC were deleted by the operator over the phone line to conserve limited receiver memory. Figure 1 shows location and instrumentation of the sites that were occupied during GPS/STORM.

Radiometrics™ WVRs are Dicke type, with a stabilized noise diode as the reference coupled in via a

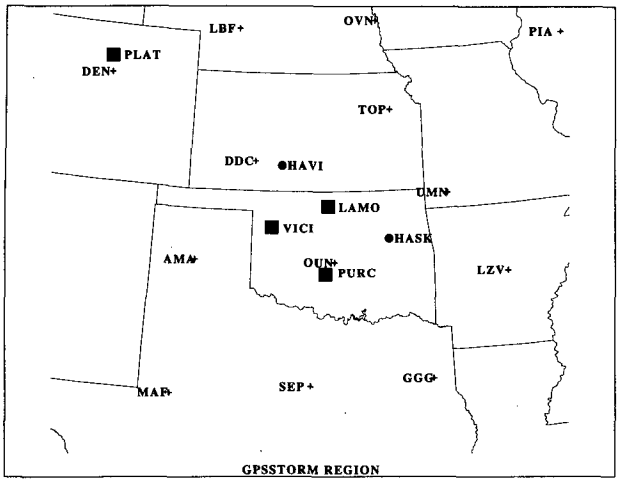

FIG. 1. Distribution of GPS sites and raobs release sites is shown. GPS sites are solid dots, GPS + WVR sites are solid squares, and raobs release sites are shown as crosses. Radiometrics™ WVRs were operated at LAMO, VICI, and PURC. PLAT has a NOAA WVR. All GPS sites, with the exception of LAMO, are NOAA wind-profiler sites. Each site was equipped with a barometer. Raobs were also released from LAMO.

Moreno cross coupler (Solheim 1993). Calibration is achieved by "tipping curves," wherein the gain of the receiver is measured by observing air masses at various elevation angles. The gain calibration is then transferred to the noise diode. Sky brightness at 23.8 and 31.4 GHz are observed, allowing both total PW and liquid water vapor to be measured. Tipping curves were automatically performed every 12 h at two orthogonal azimuths to diminish the effect of anisotropy in water vapor on calibration noise.

Liquid nitrogen cold target tests demonstrated accuracy of 0.3-K brightness and precision of 0.2 K. At an averaging time of 2 s the rms side-by-side difference in measured path delay for two Radiometrics™ WVRs is 2.9 mm; 2.1 mm are attributable to each instrument. This is consistent with 0.3-K accuracy (Ware et al. 1993).

The NOAA WVR at the reference site is described in detail by Westwater et al. (1989). During a recent experiment (Han et al. 1994), this instrument demonstrated agreement of 0.2 mm in wet delay when compared to Raman radiometric measurements. This excellent agreement was achieved under mostly dry and clear conditions, using 2-min WVR averaging.

The requirement for simultaneous availability of WVR, GPS, and barometric pressure data is the reason for data outages during our experiment and a major challenge to operational GPS PW monitoring systems. Table 1 summarizes the available data.

Pressure data are missing when the NOAA wind profilers were down. Data from the Platteville WVR are missing when upgrade work was done on that instrument during our experiment. The ARM site experienced power outages due to flooding. WVR data from Vici and Purcell (PURC) are missing due to lightning strikes that took out PC RS232 communication ports and damaged the Purcell WVR. Data loss of the Lamont (LAMO) WVR, which is operated by the ARM project, was caused by power outages. GPS data also were lost due to operator error and RS232 port problems.

4. GPS/STORM data analysis and results

a. GPS data analysis

GPS data were analyzed with the UNAVCO version of the Bernese V 3.4 software. Geodetic station coordinates were estimated for all sites in the network relative to Platteville, Colorado. These positions were computed using GPS satellite orbits generated by the Center for Orbit Determination (CODE) in Berne, Switzerland. These orbits describe the satellite positions with an rms error of better than 0.2 m. Coordinates were estimated for each day, the results were averaged, and the rms scatter of the coordinates was computed (Larson and Agnew 1991). Coordinate rms repeatability for baselines ranging from 560 to 920 km was 12–16 mm in the vertical, 5–8 mm in the horizontal baseline components, and 3–5 mm in baseline length. This rms scatter is slightly larger than expected, given the quality of the GPS orbits and data, possibly due to the high level of temporal and spatial tropospheric delay variability during our experiment. Averages of all daily solutions were used as a priori coordinates for the tropospheric delay estimation.

Differential tropospheric delay was estimated relative to the reference site, Platteville (PLAT), at the other five stations every 30 min. At times when the Platteville reference site was down due to missing GPS or missing and faulty WVR data, VICI or PURC was used as the reference site. Platteville was selected as a reference site because of its permanently operating WVR and relatively dry location.

For the tropospheric estimation, the station coordinates were also estimated within the constraints given by the rms scatter of the daily solutions. Changes in wet delay were constrained in the GPS estimation to

TABLE 1. GPS/STORM data summary.

Site	HRS* GPS	HRS pressure	HRS GPS PW	HRS WVR	HRS used for WVR–GPS comparison
VICI	626	568	495	499.7	265.5
PURC	633	616	558	486.9	299.5
LAMO	526	546	393	565.5	269.0
HASK	619	601	537	—	—
HAVI	542	630	496	—	—
PLAT	572	638	N/A	638	—

* A maximum of 660 h of data was possible for entire experiment.

1 cm h^{-1}. Tests have shown that tropospheric delay estimates are not very sensitive to these a priori constraints. GPS estimation of wet delay, as described here, does not depend critically on any a priori knowledge of the weather or its variability.

GPS software was used to estimate wet path delays at each secondary site every 30 min. Wet path delays were converted to precipitable water according to Eq. (11). Department of Defense (DoD) Selective Availability (SA) measures were activated during the experiment but did not affect the results, because we operated GPS in a differential mode (Rocken and Meertens 1991), and because we used CODE GPS orbits. DoD anti-spoofing (AS) was not on during the experiment.

b. *WVR data analysis*

NOAA processed the Platteville WVR measurements, ARM project scientists processed the data from the Radiometrics™ WVR at Lamont, and UNAVCO analyzed WVR data from Purcell and Vici. Radiometers provide verification of GPS sensing of precipitable water at the secondary sites.

Both, NOAA and Radiometrics™ WVRs measure sky brightness temperatures at two frequencies. Brightness temperatures for each frequency are converted to atmospheric opacity. This calculation depends on the mean radiating temperature as defined in Elgered (1993) as

$$T_{mr} \equiv \frac{1}{1 - e^{-\tau(s)}} \int_{\text{atm}} T(s) e^{-\tau(s)} \alpha(s) ds, \quad (15)$$

where $T(s)$ is the temperature, $\tau(s)$ is the optical depth, and $\alpha(s)$ is the absorption coefficient. Chiswell et al. (1994) discuss the estimation of T_{mr} in more detail. Using T_{mr}, the opacities at the two radiometer frequencies are calculated from

$$\tau_i = -\ln\left(\frac{T_{mr} - T_i}{T_{mr} - T_{bg}}\right), \quad (16)$$

where τ_i ($i = 1, 2$) is the opacity at frequency i, corresponding to the brightness temperature T_i, and T_{bg} is the cosmic background radiation of 2.73 K.

With known opacities the precipitable water is computed according to

$$\text{PW} = c_0 + c_1\tau_1 + c_2\tau_2, \quad (17)$$

where the c_0, c_1, and c_2 values are so-called retrieval coefficients (Elgered 1993).

The T_{mr} and retrieval coefficients were computed by linear regression analysis of radiosonde data under assumption of a model for the molecular absorption of water vapor α. NOAA estimated T_{mr} and retrieval coefficients for 20.6 and 31.65 GHz from Denver radiosonde data. ARM project scientists generated T_{mr} and retrieval coefficients at the Radiometrics™ frequencies of 23.8 and 31.4 GHz from LAMO and OUN radiosonde data.

Because T_{mr} and retrieval coefficients are site and season dependent, new sets were computed by NOAA and ARM scientists for each month of the year. Lamont values were also used at Purcell and Vici. The T_{mr} and retrieval coefficients for each day were obtained by linear interpolation of the monthly values. Appendix A provides additional information on the WVR analysis.

The inversion of *measured* WVR brightness temperatures T_i implies that these are identical to brightness temperatures *computed* from radiosonde data T_{bci}. Westwater et al. (1990) found that there is a systematic difference between the two. This was seen when NOAA WVRs were operated at radiosonde release sites. The difference is attributed to uncertainties in the water vapor absorption model. Westwater et al. (1990) found a linear relationship: $T_{bci} = a + bT_i$. We applied the correction coefficients a and b that had been estimated by NOAA for 20.6 and 31.65 GHz and by ARM scientists for 23.8 and 31.4 GHz. WVR data from Platteville are shown in Fig. 2.

c. *Radiosonde data analysis*

Raob analysis was done at NCSU. Integrated water vapor is calculated from National Weather Service twice-daily radiosonde launches by the formula

$$\text{IWV} = \int \rho_v dz, \quad (18)$$

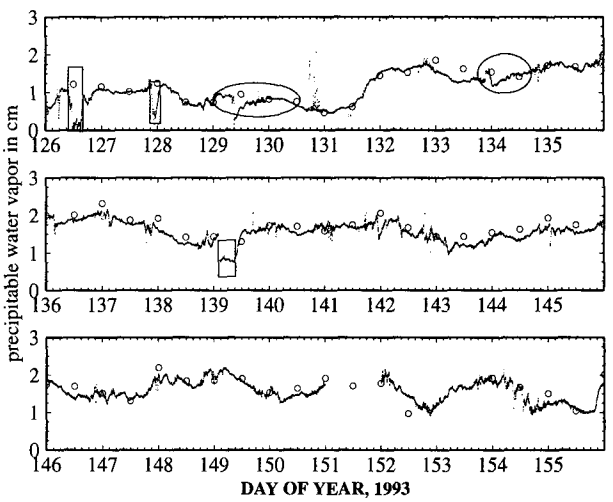

FIG. 2. WVR data from Platteville and raobs from Denver at a distance of 50 km are shown. The PW burden at all other sites of the network is computed relative to these WVR values. Areas of bad WVR measurements, due to unexplained instrumental errors and service work that was performed on the instrument during the experiment, are "boxed." Data during these times were not included in the GPS–WVR comparison. "Circled" areas indicate missing GPS data at Platteville. During these times either Vici or Purcell were used as reference sites.

where ρ_v is the density of water vapor and the integral is computed along a path through the atmosphere. Precipitable water is then

$$\mathrm{PW} = \frac{\mathrm{IWV}}{\rho_w}, \tag{19}$$

where ρ_w is the density of liquid water. The partial pressure of water vapor P_v at each level in the sounding is calculated from the dewpoint, temperature, and pressure. Vapor density is then computed as

$$\rho_v = \frac{P_v}{R_v T}, \tag{20}$$

where R_v is the gas constant for vapor.

Once ρ_v values are calculated for each level in the sounding, IWV is calculated by summing the mean water vapor density ρ_v in each layer:

$$\mathrm{IWV} = \sum \overline{\rho_v} dz, \tag{21}$$

where $\overline{\rho_v} = 0.5(\rho_1 + \rho_2)$ and $dz = z_2 - z_1$, and where the subscripts 1 and 2 denote the top and bottom of each layer.

NWS soundings consist of mandatory reports at 1000, 925, 850, 700, 500, 400, 300, 250, 200, 150, and 100 mb. There are other mandatory levels above 100 mb, but up until November 1992 United States soundings did not report dewpoint at temperatures lower than −40°C, due to the procedure established for the 1950s vintage hygristors (Wade 1994). These hygristors are no longer used, allowing reporting of dewpoint (relative humidity) to greater altitudes. In general, however, the contribution of water vapor above the tropopause is very small.

Values of PW were calculated at all North American radiosonde sites. Objective analysis in the domain of the radiosonde sites was performed to interpolate the data to a regular grid. The gridded data were used to interpolate (via bilinear interpolation) values to locations where radiosonde launches are not available. This interpolation had to be done for all GPS/STORM sites, except Lamont, which was the only GPS/WVR site collocated with an raob release site.

d. *Combining GPS, WVR, and barometric pressure data*

Platteville WVR and barometric pressure data were used to compute a priori total tropospheric delays for each GPS observation. WVR and pressure measurements were interpolated to each 30-s GPS measurement epoch. Interpolated WVR values were converted from precipitable water to zenith delay using interpolated surface temperature data. Zenith wet delay values were scaled to the elevation of each GPS satellite. Pressure measurements and the Saastamoinen model (1972) and mapping function determined the hydrostatic delay in the direction of each GPS satellite. The sum of hydrostatic delay plus wet delay corrections were applied to each GPS observation at the reference site, Platteville.

e. *Results*

GPS data analysis yielded 30-min estimates of zenith wet delay for all five secondary stations in the GPS/STORM network. These 30-min estimates were converted to precipitable water and compared to independent WVR measurements at Lamont, Vici, and Purcell. Results were also compared to radiosonde estimates at all five secondary sites.

Figure 3 shows results for GPS/STORM. For the comparison of GPS and WVR estimates it is necessary to identify and exclude sections of bad WVR observations. WVR data are not reliable when liquid water is present on the WVR reflector (NOAA) or window (Radiometrics™). The Platteville WVR (Fig. 2) is less sensitive to this problem because it uses a rapidly rotating reflector that tosses water droplets off, drying itself through centrifugal action. Periods of faulty WVR data were identified by several criteria. Surface meteorological records identified periods of high humidity and rain. In addition, liquid water forming on the window of the Radiometrics™ WVR can be detected by sharp gradients in measured brightness temperatures and by brightness temperatures above 100 K.

GPS and WVR results in Fig. 3 are in good agreement. Raob data agree with GPS and WVR at Lamont and Purcell, presumably because these GPS/STORM sites are close to radiosonde release sites. Not surprisingly, agreement between interpolated radiosonde data and GPS or WVR at the other sites is worse.

Comparison of WVR and GPS estimates of precipitable water for the entire experiment is summarized in Table 2. Since each GPS estimate of the wet delay is based on 30 min of GPS data, we compare this GPS estimate to WVR data collected during the same 30 min. WVR observations were scaled to zenith (required only for the pointed WVR observations from Purcell and Vici) and averaged. This is an average of observations that vary in time and direction. The rms scatter of these WVR averages contributes to the noise in the WVR–GPS comparison and is, therefore, listed in the last column of Table 2. Note that this rms is much lower at Lamont (0.3 mm) than at Vici and Purcell, because the Lamont WVR observed in the zenith direction only and did not measure the directional variability of PW.

The results in Table 2 show that the rms agreement between WVR and GPS estimates of precipitable water ranged from 1.2 to 1.8 mm for the GPS/STORM experiment. These rms differences include GPS errors, WVR errors, and hydrostatic delay errors at reference and secondary sites.

f. *Discussion of results*

For GPS/STORM we report an rms difference of approximately 1.5 mm between GPS and WVR esti-

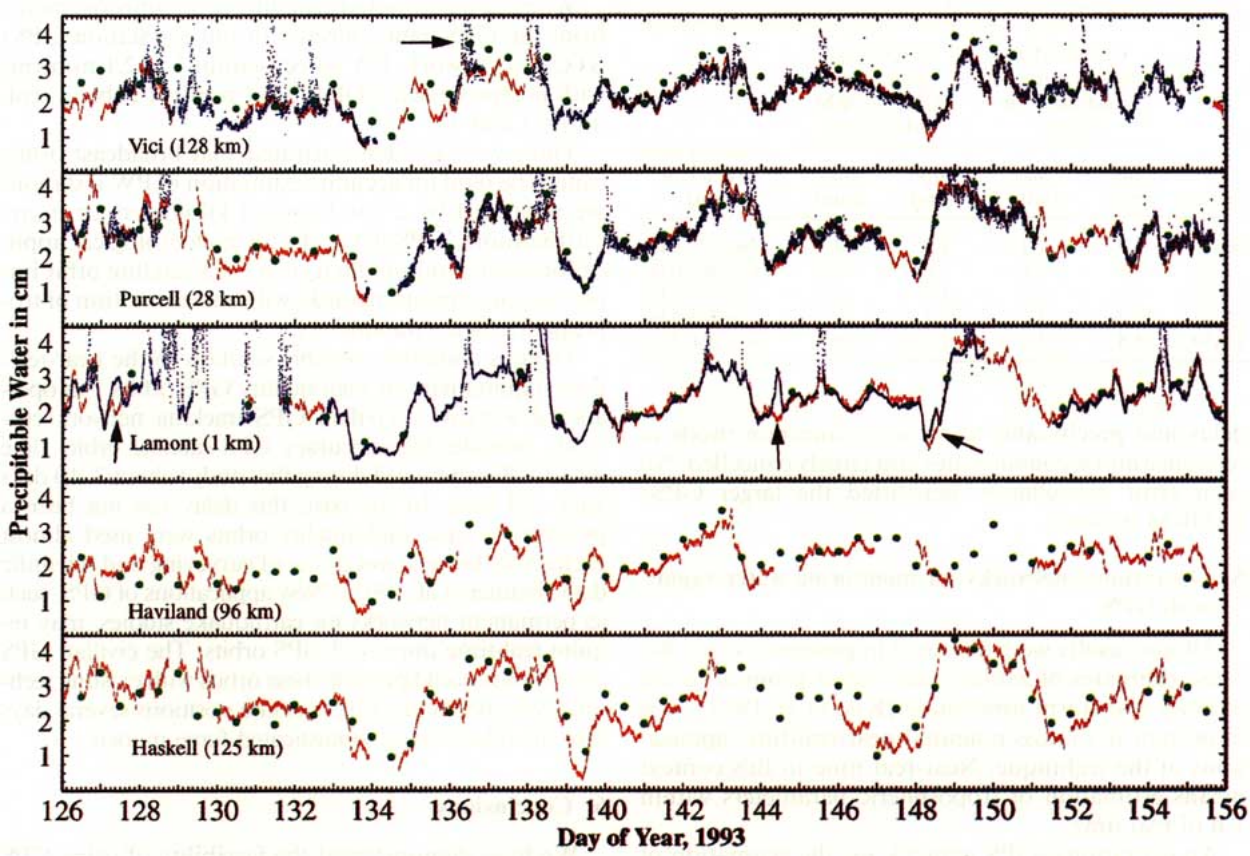

FIG. 3. Precipitable water (PW) is shown for 30 days and five stations. Each panel shows the station name and distance from nearest roab release site in the lower left corner. Small blue dots in the top three traces of each panel are WVR measurements, small red vertical lines are 30-min GPS estimates, and the isolated green points are from raobs. WVRs at VICI and PURC were pointed at the GPS satellites, and the measurements were scaled to zenith. The Lamont WVR observed in the zenith direction only. The arrows in the Lamont panel point at examples of faulty WVR data—in these cases caused by dew on the WVR window. The arrow in the top panel indicates rain.

mates of precipitable water at the secondary sites. As was discussed earlier in this paper, we expect a zenith wet path delay error of about 8 mm for the GPS differential estimation relative to a reference site. This corresponds to an error of about 1.2 mm in precipitable water. More than half of this error (6-mm error in path delay or about 1 mm in precipitable water) can be attributed to WVR errors at the reference site.

Because the WVR at the secondary site must be expected to have an error similar to the reference WVR, these errors combine to a GPS–WVR comparison error as $\text{rms}_{\text{error}} = (8^2 + 6^2)^{1/2} = 10$ mm. This 10-mm error in path delay corresponds to 1.5 mm uncertainty in precipitable water. Observed differences range from 1.2 to 1.8 mm, in some cases larger than the expected error, presumably because of the additional uncertainty due to spatial and temporal averaging of the WVR measurements during each 30-min GPS solution interval.

Rocken et al. (1993) reported submillimeter agreement for a similar GPS–WVR comparison near Boulder, Colorado. There are several reasons for the superior WVR–GPS agreement in that study. First, we used two identical Radiometrics™ WVRs. Furthermore, these WVRs were operated only 50 km apart under similar climatic conditions. Thus, errors incurred when converting WVR brightness temperatures to wet

TABLE 2. Comparison of WVR and GPS precipitable water.

Site	No. of points (1 point per 30 min)	WVR − GPS rms (mm)	GPS − WVR bias (mm)	WVR − GPS bias removed rms (mm)	WVR temporal and spatial rms (mm)
LAMO	538	1.59	0.80	1.39	0.3
VICI	531	1.20	−0.01	1.20	1.2
PURC	599	1.81	0.04	1.77	1.2

TABLE 3. Precipitable water comparison for different GPS orbits.

Station	CODE orbit results minus broadcast orbit results: rms (mm)	CODE orbit results minus broadcast orbit results: Bias (mm)	CODE orbit results minus GPS/STORM orbit results: rms (mm)	CODE orbit results minus GPS/STORM orbit results: Bias (mm)	Distance from Platteville (m)
HAVI	3.3	2.1	1.3	0.1	562 272.981
VICI	3.9	2.6	1.6	−0.3	663 962.078
LAMO	4.4	3.7	1.6	0.2	745 807.938
PURC	5.4	3.7	2.1	0.2	858 285.746
HASK	5.4	3.7	1.9	−0.3	922 066.382

delay and precipitable water were common mode at reference and secondary sites and largely cancelled. No such error cancellation benefitted the larger GPS/STORM network.

5. Operational networks for monitoring water vapor with GPS

All our results were obtained in postprocessing. Because estimates of zenith water vapor promise to aid weather and storm forecasting (Kuo et al. 1993), it is important to discuss potential near-real-time applications of the technique. Near-real time in this context means estimation of tropospheric parameters within 1 h of real time.

An operational GPS network for the estimation of meteorological parameters must have the communications infrastructure to download the latest 30 min of GPS data to a processing center. Thirty minutes of GPS data, sampled at 30 s, are about 15 kbyte, if compressed. Pressure and surface temperature from all sites must also be communicated to the processing center.

Differential estimation requires at least one reference WVR and barometer or other means to measure a priori total tropospheric delay. Because of WVR data problems during rain, the reference site should be located in an arid region. To avoid outage of the entire network and for redundancy checks, two or three reference sites may be desirable for operational GPS meteorological networks.

The size of the network determines the requirements for GPS satellite orbit quality. Small-scale networks of approximately 50 km can determine millimeter-level precipitable water, using on-line GPS broadcast orbits. These orbits are good enough for small networks because orbit errors affect all stations similarly and, thus, largely cancel. Broadcast orbits do not suffice for networks spanning larger distances as demonstrated in Table 3.

Table 3 shows the rms difference in GPS estimated PW for different satellite orbits. Note that broadcast orbit results differ by up to 5.4 mm from results with improved CODE orbits (column 1) and that they are significantly biased (column 2). These errors increase with distance from the reference site Platteville (column 5).

When we computed satellite orbit improvements from the GPS data collected in our six-station GPS/STORM network, PW agrees within 1.3–2.1 mm rms with postprocessed CODE orbit results (Table 3, columns 3 and 4).

Thus, we have demonstrated that broadcast orbits cannot be used for accurate estimation of PW if stations are separated by a few hundred kilometers or more. Furthermore, GPS networks for meteorological applications can compute their own GPS satellite orbit improvements simultaneously with the estimation of tropospheric delay parameters.

There is a another possible solution to the near-real-time requirement for high-quality GPS orbits. An operational worldwide civilian GPS tracking network currently provides high-accuracy GPS satellite orbits (like the CODE orbits used during this study) about 7–10 days after real time. In the past, this delay has not been a problem because high-quality orbits were used almost exclusively for postprocessing of surveying and scientific data (Beutler et al. 1993). New applications of GPS, such as permanent networks for earthquake studies, may require real-time improved GPS orbits. The civilian GPS community could provide these orbits with existing technology by predicting GPS satellite positions several days into the future using sophisticated force models.

6. Conclusions

We have demonstrated the feasibility of using GPS to monitor atmospheric water vapor with 1–2-mm accuracy over a 900-km, six-receiver network. These are promising results, and future research shall focus on three main areas.

First, we must assess the meteorological value of high-resolution, high-accuracy values of precipitable water. This study could examine the effect of the GPS/STORM precipitable water time series on numerical weather forecasts.

We shall also investigate the feasibility of operating near-real-time GPS meteorological monitoring networks. This will require software development and testing for GPS orbit prediction, data communication links, and automated GPS data processing.

Finally, the accuracy of GPS-estimated precipitable water shall be improved. A large part of the uncertainty is due to WVR errors at the reference site. Improvement of WVR retrieval algorithms and techniques is one way to reduce this error. Alternatives to WVRs must also be investigated. This paper discussed absolute tropospheric parameter estimation with GPS and barometers. We tested absolute estimation with the GPS/STORM data and found the agreement with WVRs to be 15% worse than for differential processing. Methods to improve absolute estimation algorithms and strategies are currently under investigation. GPS errors can also be reduced with improved hardware and software. Better GPS antennas can be installed at the sites

to reduce GPS multipath effects on tropospheric estimation (Rocken et al. 1993).

The GPS techniques that were used in this study to estimate water vapor in the atmosphere were originally developed by geodesists and geophysicists to improve vertical surveying accuracies with GPS. We believe that continued cooperation between geophysicists and atmospheric scientists will result in GPS networks that provide the highest surveying accuracies and resolution for solid earth studies, in addition to atmospheric water vapor, for improved weather and storm forecasting.

Acknowledgments. Thanks to Dr. Russ Chadwick, Seth Gutman, and others from the NOAA wind profiler group for logistical support during GPS/STORM. Dr. Ed Westwater and Michael Falls from NOAA/ETL provided retrieval coefficients and WVR data from Platteville. Thanks to Dr. James Lijegren and the ARM project for support at the CART site and for Lamont WVR data. Radiometrics™ Inc. of Boulder loaned two WVRs for this work. NSF Grant ATM-9204076 provided support. UNAVCO with NSF support under Grant EAR-9116461 provided data analysis facilities, GPS equipment, and field support. UNAVCO staff Jim Normandeau, John Braun, and Chris Alber worked long hours in the field, as did Jing-Ping Duan from NCSU.

APPENDIX

Summary of the Constants Used for Processing WVR Data

a. Radiometrics™ WVR data analysis

Table A1 summarizes retrieval coefficients and values of T_{mr} used for the analysis of Radiometrics™ WVR data using Eqs. (16) and (17).

We assumed the values to apply to the middle of each month (i.e., 15 April). For the days between 15 April and 15 May, and between 15 May and 15 June, we obtained daily values by linear interpolation.

Measured brightness temperatures were tuned, to correct for errors in molecular absorption models, according to the equation $T_{bci} = a + bT_i$. The tuning constants that we used are given in Table A2.

TABLE A1. Radiometrics™ retrievals and T_{mr} values.

Month	c_0	c_1	c_2	T_{mr23}	T_{mr31}
April	0.051116	22.070	−12.531	278.636	275.247
May	0.051971	22.455	−12.829	282.634	279.721
June	0.072164	22.449	−12.717	285.446	283.021

TABLE A2. Radiometrics™ tuning coefficients.

Frequency (GHz)	a	b
23.8	1.3066	0.904
31.4	1.1923	0.910

TABLE A3. NOAA Platteville retrievals and T_{mr} values.

Month	c_0	c_1	c_2	T_{mr20}	T_{mr30}
April	0.017312	27.987	−12.175	267.086	263.330
May	0.026868	28.104	−12.190	271.352	267.452
June	0.022992	28.600	−12.369	275.926	272.021

TABLE A4. NOAA Platteville WVR tuning coefficients.

Frequency (GHz)	a	b
20.60	0.263	0.863
30.65	−0.719	0.982

These tuning coefficients account for errors in the absorption line model used to generate the c_0, c_1, and c_2 retrieval coefficients from several years of historical raobs. ARM project scientists computed these tuning coefficients from linear regression of brightness temperatures, calculated from raobs at Lamont, using NOAA's microwave radiation transfer model by Schroeder and Westwater (1991), against brightness temperatures measured with the Radiometrics™ WVR at the Lamont ARM site over a period of 18 months.

b. NOAA WVR data analysis

NOAA retrieval coefficients and T_{mr} values are summarized in the following table. The retrieval coefficients for each month are 3-month averages. Thus, the values for May are computed from April, May, and June raobs. June's values are computed from raobs collected during May, June, and July. Monthly values were applied by NOAA without any interpolation.

Note that April coefficients, given in Table A3, were not used for the analysis of GPS/STORM data because NOAA's WVR analysis does not interpolate between monthly retrieval coefficients.

Table A4 shows the NOAA tuning coefficients that were used for the analysis.

REFERENCES

Beutler, G., P. Morgan, and R. E. Neilan, 1993: Geodynamics: Tracking satellites to monitor global change. *GPS World,* **4,** 40–46.

Bevis, M., S. Businger, T. A. Herring, C. Rocken, R. A. Anthes, and R. H. Ware, 1992: GPS meteorology: Remote sensing of atmospheric water vapor using the global positioning system. *J. Geophys. Res.,* **97,** 15 787–15 801.

——, ——, S. R. Chiswell, T. A. Herring, R. A. Anthes, C. Rocken, and R. H. Ware, 1994: GPS meteorology: Mapping zenith wet delays onto precipitable water. *J. Appl. Meteor.,* **33,** 379–386.

Boudouris, G., 1963: On the index of refraction of the air, the absorption and dispersion of centimeter waves by gasses. *J. Res. Nat. Bur. Sta., Sec D,* **67,** 631–684.

Chiswell, S., S. Businger, M. Bevis, F. Solheim, C. Rocken, and R. H. Ware, 1994: The impact of mean radiating temperature in retrieval of integrated water vapor from water vapor radiometer measurements. *J. Atmos. Oceanic Technol.*, submitted.

Davis, J. L., T. A. Herring, I. L. Shapiro, A. E. E. Rogers, and G. Elgered, 1985: Geodesy by radio interferometry: Effects of atmospheric modeling errors on estimates of baseline length. *Radio Sci.*, **20,** 1593–1607.

Elgered, G., 1993: Tropospheric radio-path delay from ground-based microwave-radiometry. *Atmospheric Remote Sensing by Microwave Radiometry,* Wiley, 215–258.

Gary, B. L., S. J. Keihm, and M. A. Janssen, 1985: Optimum strategies and performance for the remote sensing of path-delay using ground-based microwave radiometers. *IEEE Trans. Geosci. and Remote Sens.*, **GE-23,** 479–484.

Han, Y., J. B. Snider, E. R. Westwater, S. H. Melfi, R. A. Ferrare, 1994: Observations of water vapor by ground-based microwave radiometers and raman lidar. *J. Geophys. Res.*, **99,** 18 695–18 702.

Herring, T. A., 1986: Precision of vertical position estimates from very long baseline interferometry. *J. Geophys. Res.*, **91,** 9177–9182.

Hopfield, H. S., 1971: Tropospheric effect on electromagnetically measured range: Prediction from surface weather data. *Radio Sci.*, **6,** 357–367.

Kuo, Y.-H., Y.-R. Guo, and E. R. Westwater, 1993: Assimilation of precipitable water measurements into mesoscale numerical models. *Mon. Wea. Rev.*, **121,** 1215–1238.

Larson, K. M., and D. Agnew, 1991: Application of the Global Positioning System to crustal deformation measurement: 1. Precision and accuracy. *J. Geophys. Res.*, **96**(B10), 16 547–16 565.

Remondi, B. W., 1984: Using the GPS phase observable for relative geodesy: Modelling, processing, and results. Ph.D. thesis, University of Texas, 360 pp.

Rocken, C., and C. M. Meertens, 1991: Monitoring selective availability dither frequencies and their effect on GPS data. *Bull. Geod.*, **65,** 162–169.

——, R. H. Ware, T. van Hove, F. Solheim, C. Alber, J. Johnson, M. Bevis, and S. Businger, 1993: Sensing atmospheric water vapor with the global positioning system. *Geophys. Res. Lett.*, **20**(23), 2631–2634.

Rothacher, M., 1992: Orbits of satellite systems in space geodesy. *Geodaetisch-geophysikalische Arbeiten in der Schweiz,* Vol. 46, Schweizerischen Geodaetischen Kommission, 243 pp.

Saastamoinen, J., Atmospheric correction for the troposphere and stratosphere in radio ranging of satellites. *The Use of Artificial Satellites for Geodesy,* Geophys. Monogr. Ser., Vol. 15, Amer. Geophys. Union, 247–251.

Schroeder, J. A., and E. R. Westwater, 1991: User's guide to WPL microwave radiometric transfer software. NOAA Tech. Memo. ERL WPL-213, 84 pp.

Smith, E. K., and S. Weintraub, 1953: The constants in the equation for atmospheric refractive index at radio frequencies. *Proc. IRE,* 1035–1037.

Solheim, F. S., 1993: Use of pointed WVR observations to improve vertical GPS surveying accuracy. Ph.D. thesis, University of Colorado, 128 pp.

Spilker, J. J., 1980: Signal structure and performance characteristics. *Global Positioning System: Papers Published in Navigation,* P. M. Janiczek, Ed., 29–54.

Tralli, D. M., and S. M. Lichten, 1990: Stochastic estimation of tropospheric path delays in global positioning system geodetic measurements. *Bull. Geod.*, **64,** 127–159.

——, ——, and T. Herring, 1992: Comparison of Kalman filter estimates of zenith atmospheric path delays using GPS and VLBI. *Radio Sci.*, **27,** 999–1007.

Wade, C. G., 1994: An evaluation of problems affecting the measurement of low relative humidity on the United States radiosonde. *J. Atmos. Oceanic Technol.*, **11,** 687–700.

Ware, R. H., C. Rocken, F. Solheim, T. van Hove, C. Alber, and J. Johnson, 1993: Pointed water vapor radiometer corrections for accurate global positioning surveying. *Geophys. Res. Lett.*, **20**(23), 2635–2638.

Westwater, E. R., 1978: The accuracy of water vapor and cloud liquid determination by dual-frequency ground-based radiometry. *Radio Sci.*, **13,** 677–685.

——, M. J. Falls, and I. A. Popo Fotino, 1989: Ground-based microwave radiometric observations of precipitable water vapor: A comparison with ground truth from two radiosonde observing systems. *J. Atmos. Oceanic Technol.*, **6,** 724–730.

——, J. B. Snider, and M. J. Falls, 1990: Ground-based radiometric observations of atmospheric emission and attenuation at 20.6, 31.65, and 90 GHz: A comparison of measurement and theory. *IEEE Trans. Antennas Propag.*, **38,** 1569–1580.

Yuan, L., R. A. Anthes, R. H. Ware, C. Rocken, W. D. Bonner, M. G. Bevis, and S. Businger, 1993: Sensing climate change using the Global Positioning System. *J. Geophys. Res.*, **98**(D8), 14 925–14 937.